

PAPER

## Equal channel angular pressing of spheroidal graphite cast iron

To cite this article: J Bahadori-Fallah *et al* 2019 *Mater. Res. Express* **6** 066542

View the [article online](#) for updates and enhancements.



**IOP | ebooks™**

Bringing you innovative digital publishing with leading voices to create your essential collection of books in STEM research.

Start exploring the collection - download the first chapter of every title for free.



## PAPER

## Equal channel angular pressing of spheroidal graphite cast iron

RECEIVED  
7 February 2019REVISED  
27 February 2019ACCEPTED FOR PUBLICATION  
7 March 2019PUBLISHED  
22 March 2019J Bahadori-Fallah, M H Farshidi  and A R Kiani-Rashid

Department of Materials Science and Metallurgical Engineering, Ferdowsi University of Mashhad, Mashhad, Iran

E-mail: [farshidi@um.ac.ir](mailto:farshidi@um.ac.ir)**Keywords:** equal channel angular pressing, spheroidal graphite cast iron, warm deformation, severe plastic straining**Abstract**

Spheroidal graphite cast iron is an engineering material which has proved its importance during previous decades. However, limited workability of this material could be a challenge for spreading of its applications and there is a little knowledge about severe straining of this material at warm and/or cold regimes. This work is conducted to examine imposition of a well-known severe plastic deformation process called equal channel angular pressing on this material through a warm deformation regime. For this purpose, a casing procedure combined with an pre-annealing treatment is applied to increase the workability of this material. Results show that an equivalent plastic strain as great as 0.9 can be successfully imposed on the spheroidal graphite cast iron at a temperature lower than half of the melting temperature of iron while no evidence from dynamic recrystallization of the ferrite phase is traced. This enhanced warm workability of SG cast iron is related to imposition of a compressive stress state as well as decrease of pearlite fraction by the pre-annealing.

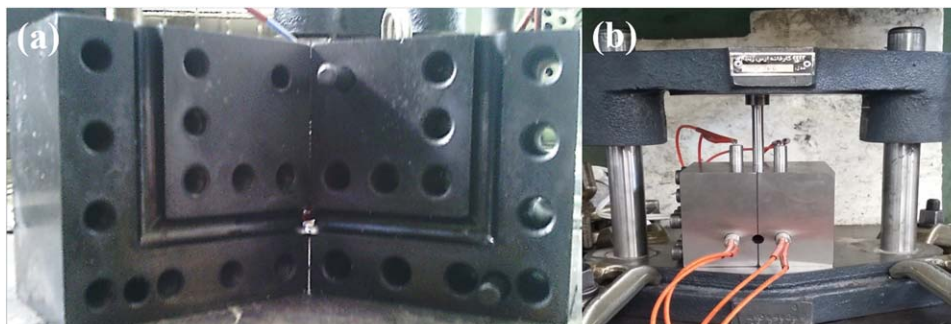
**1. Introduction**

Nowadays, grey cast irons are still attractive due to their exclusive characteristics such as low price, good corrosion resistance, good machinability, self-lubrication and good castability. However, the toughness and the ductility of conventional grey cast iron are relatively poor which restrict its applications. This is due to the planar shape of graphite phase in this material which stimulates its fracture during deformation. To reduce this weakness of the conventional grey cast iron, Spheroidal Graphite (SG) cast iron was introduced during the middle of 20th century by addition of a negligible amount of Mg [1–3]. In comparison of the conventional grey cast iron, SG cast iron shows a considerable increase of toughness owing to sphere-shape of its graphite phase. However, the workability of SG cast iron has still remained poor and this alloy can hardly bear plastic strain equal to 10% at ambient temperature. Therefore, there has been only one solution for increasing workability of this alloy: applying a hot deformation regime. For more explanation, when  $T_m$  is considered as the melting temperature of a metal, the hot deformation is considered as the deformation at a temperature above  $0.5-0.6T_m$  and less than  $T_m$ . This enhanced temperature of deformation causes activation of diffusion dependent phenomena like dynamic recrystallization and as a result, it increases the workability of the metal by slowing down the fracture mechanisms [4, 5]. Although the hot deformation of SG cast iron was relatively successful [3, 6–10], one may request deformation of this alloy at lower temperatures. One reason might be that occurrence of the dynamic recrystallization and its subsequent grain growth may cause softening of the material [10–12]. In addition, applying of a hot deformation regime for iron usually causes occurrence of austenite to ferrite transformation after the deformation which could be undesirable [1, 3]. Despite these considerations about applying of hot deformation regime for the SG cast iron, applying of a warm/cold deformation regime for this alloy is almost neglected in previous studies on this topic.

Successful plastic deformation of metals and alloys with poor workability requires imposing of a considerable hydrostatic pressure during deformation since the hydrostatic pressure causes deceleration of the void growth/coalescence fracture mechanism [12–15]. While imposing of the hydrostatic pressure could be achieved in different ways, it is usually unavoidable to apply a compressive deformation process like the rolling or the forging. One of the compressive deformation processes often applied for thermomechanical processing of

**Table 1.** Chemical composition of the SG cast iron used in this work.

Element	Mg	S	P	Sn	Mn	Si	C	Fe
Concentration (wt%)	0.051	0.056	0.027	0.016	0.39	2.9	3.31	Rem.

**Figure 1.** Manufactured ECAP/E die used in this work: (a) opened and (b) assembled. In (b), wires are connected to electrical heating elements.

metals and alloys with poor workability is Equal Channel Angular Pressing/Extrusion (ECAP/E) [15–17]. However, while previous studies have tried different compressive deformation processes on SG cast iron [3, 6–10], ECAP/E processing of this alloy has been remained neglected.

This study is focused on ECAP/E processing of SG cast iron at a warm deformation temperature. For this purpose, different types of casing are applied on this alloy to assist increase of its workability while the processing temperature is remained constant. After successful ECAP/E processing of SG cast iron, a hardness measurement and different microstructural studies are applied for realizing effect of the process on the variations of microstructure and hardness of the alloy. Results of these studies provide a better understanding from workability of SG cast iron at the warm temperature regime.

## 2. Process, material and experiments

SG cast iron is produced by casting of a melt prepared using iron scraps, Fe-Si and Fe-Si-Mg alloyants. The chemical composition of produced cast iron shown in table 1 is obtained by spark emission spectroscopy. After the casting step, two groups of samples are prepared: as cast samples and annealed samples. For annealing of the second group, they are subjected to 1 h of annealing at 1173 °K and then, their temperature is reduced by the rate of 110 °K h<sup>-1</sup> to 973 °K. These samples are remained at 973 °K for 1 h and then, they are cooled by the rate 55 °K h<sup>-1</sup>.

An ECAP/E die for circular rods with diameter of 10 mm is manufactured using D2 steel. As shown in figure 1(a), the channel angel of manufactured die is 90° while its corner radius is 2.5 mm. The ECAP/E processing is accomplished at 823 °K which is about 0.45 of melting temperature of the iron. For this purpose, four electrical heating elements are inserted to the die as shown in figure 1(b). In order to reduce the probability of fracture of cast iron during the process, two different alloys are used for casing of the cast iron: yellow brass and CK45 steel. For this purpose, cast iron is machined to 4 mm diameter rods and then, these rods are pushed to the seamless casing tubes prepared form mentioned alloys. The outer diameter of casing tubes is 10 mm while their thickness were 3 mm. Figures 2(a) and (b) shows a typical cast iron rod and its casing. The length of the specimens is considered equal to 65 mm and MoS<sub>2</sub> aerosol is used for lubrication of die/specimen surfaces.

To investigate effects of ECAP/E processing on microstructural evolution of SG cast iron, specimens are cut into two parts along their length. Then, specimens are subjected to mechanical polishing and etching for observation using Optical Microscope (OM) and Scanning Electron Microscope (SEM). As shown in figure 2(c), the microstructural investigations are accomplished in two different regions of specimens: the first region placed in the middle of specimen and the second region placed with a 5 mm distance from the head of specimen. In order to obtain an accurate assumption from the changes of graphite shape through ECAP/E process, MIP4 image analysis software is used. In addition, effect of ECAP/E processing on the hardness of cast iron is measured through Rockwell A hardness measurement inside two different regions of specimen.

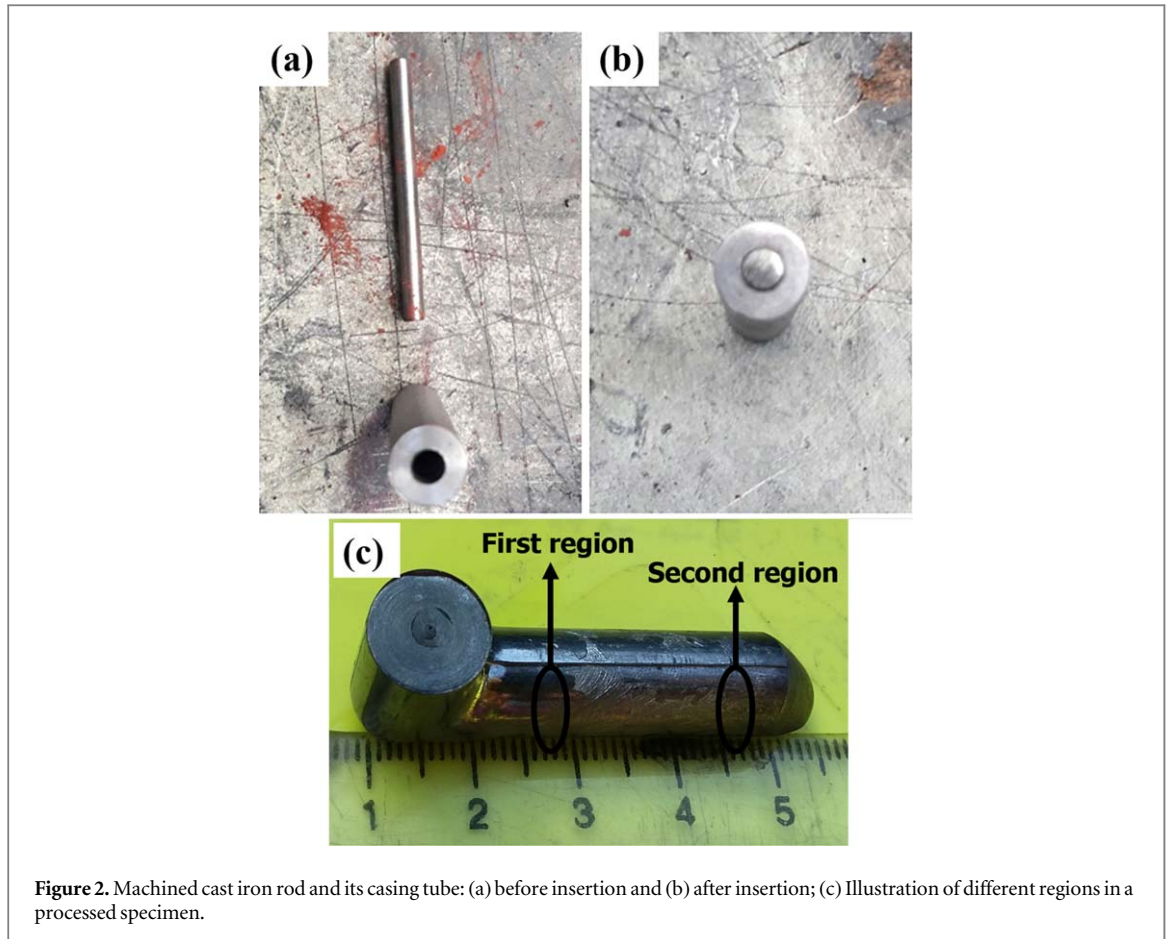


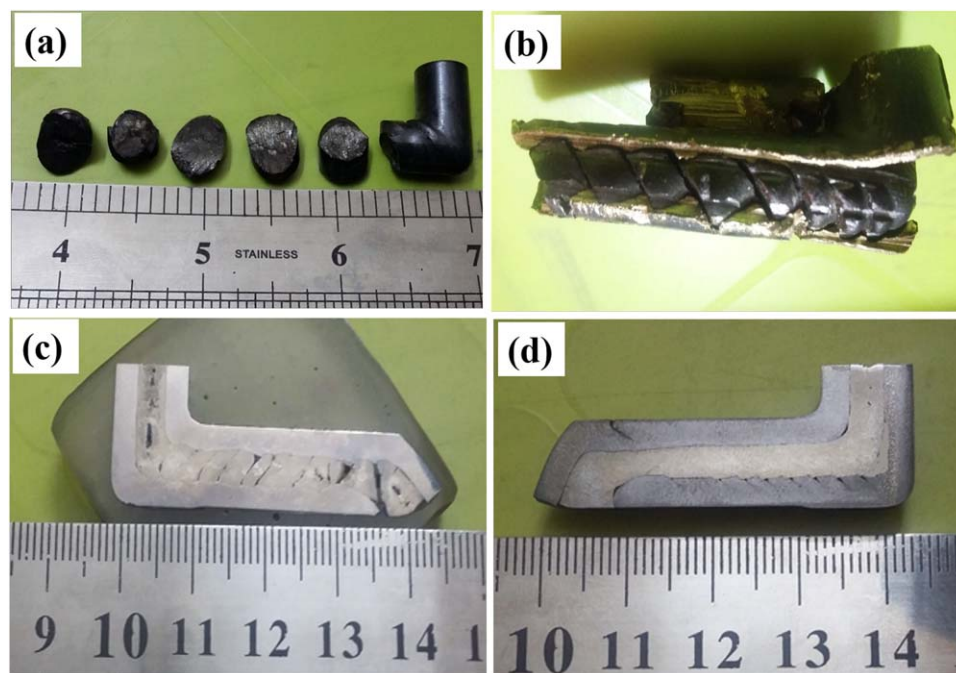
**Figure 2.** Machined cast iron rod and its casing tube: (a) before insertion and (b) after insertion; (c) Illustration of different regions in a processed specimen.

### 3. Results and discussion

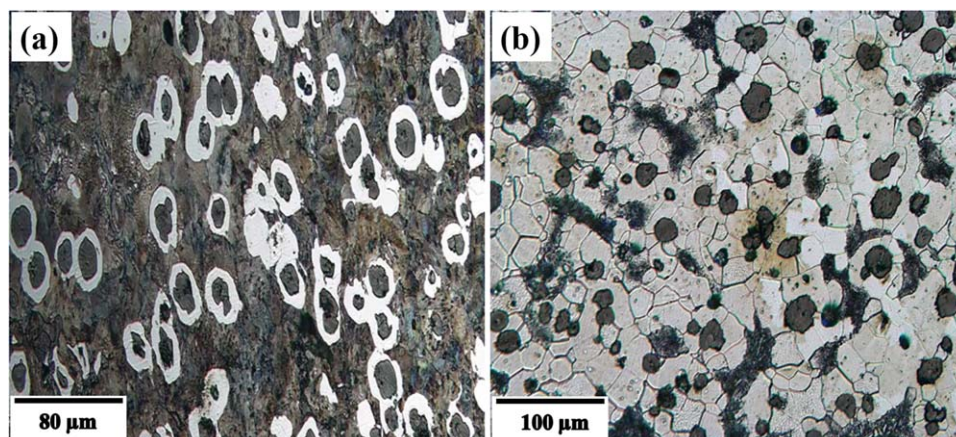
Figure 3 compares effect of application of casing on preventing of fracture during ECAP/E processing. As shown here, SG cast iron without casing is fractured during the process and application of a casing from yellow brass is not successful in preventing of fracture of this material during the process. Comparatively, CK45 steel casing is relatively successful in preventing of fracture during the ECAP/E process. This is more obvious for the annealed specimen whereas no macroscopic crack can be seen after the process. This result implies that the successful ECAP/E processing of annealed SG cast iron not only is related to use of a suitable casing, but also is a result of appearance of a more ductile microstructure during the annealing. As can be seen in figure 4, about 65% of the microstructure of as cast specimen is pearlite while the remained fraction consists of ferrite and spheroidal graphite. This microstructure appears due to rapid cooling after the casting process which allows formation of the pearlite instead of the graphite and the ferrite [1, 3]. Comparatively, less than 20% of pearlite has remained inside the microstructure after the annealing treatment and the majority of pearlite has decomposed to the ferrite and the spheroidal graphite. Therefore, one can infer that the fracture of as cast specimen during the process is related to its more brittle microstructure containing a higher fraction of pearlite since the pearlite is more brittle than the two other phases [1, 10]. Considering figure 4, it is also notable that the ferrite grains are equiaxed while graphite particles are almost spheroidal before the process.

Figure 5 compares shapes of graphite particles of annealed specimen before and after the ECAP/E process. As can be seen here, while the shapes of graphite particles before the process are almost spheroidal, the shapes of these particles after the process are completely different. For more explanation, the graphite particles are stretched during the process and their aspect ratios are increased. Similar results have been reported in previous studies on deformation of SG cast iron [6–10]. It is also notable that the aspect ratios of graphite particles in the first region of specimen are greater than their counterparts in the second region. The shape of graphite particles before and after the ECAP/E process can be simplified to sphere and elliptic, respectively. Considering this simplification, one can relate imposed principal plastic strains to the dimensions of graphite particles as below:

$$\varepsilon_1 = Ln\left(\frac{b}{d}\right) \quad (1)$$



**Figure 3.** Appearance of the cast iron subjected to ECAP/E process: (a) without casing, (b) with yellow brass casing, (c) and (d) with Ck45 casing. Figures (a) to (c) are related to the as cast specimen while (d) is related to the annealed specimen.



**Figure 4.** Microstructure of SG cast iron before the ECAP/E process: (a) as cast and (b) annealed.

$$\varepsilon_3 = \ln\left(\frac{a}{d}\right) \quad (2)$$

Here,  $\varepsilon_i$  are imposed principal plastic strains,  $d$  is the diameter of graphite sphere before the ECAP/E process while  $a$  and  $b$  are the smaller and the larger diameters of graphite elliptic after the process, respectively. Considering the cylindrical shape of specimens which causes a three dimensional strain field, neither plane strain formulation nor axisymmetric strain formulation can be applied for the used ECAP/E process [18, 19]. However, one may consider the second principal strain as below:

$$\varepsilon_2 = \alpha\varepsilon_3 \quad (3)$$

Regarding the volume constancy, one can see that:

$$\varepsilon_1 + \varepsilon_2 + \varepsilon_3 = \varepsilon_1 + (1 + \alpha)\varepsilon_3 = 0 \quad (4)$$

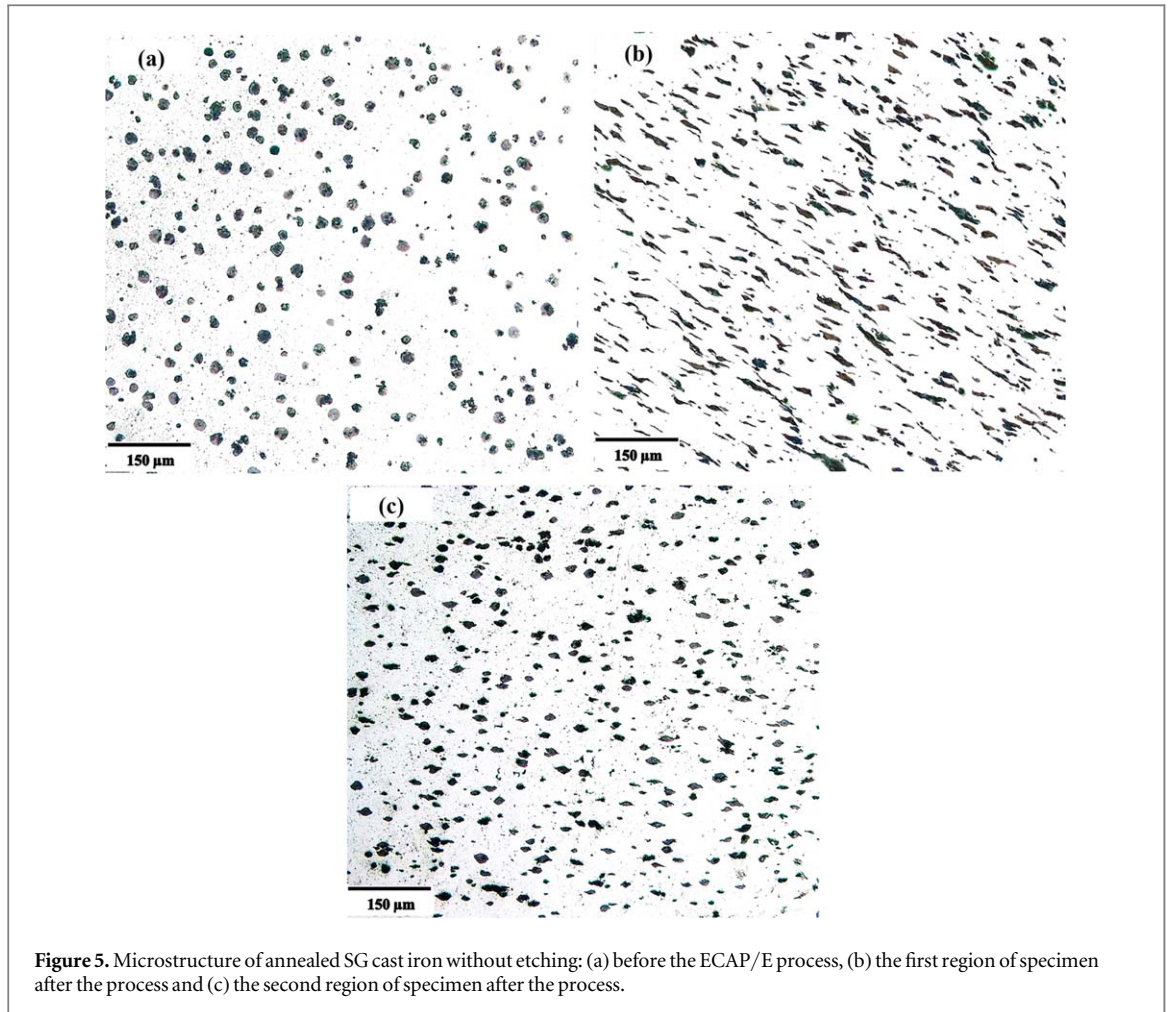


**Figure 5.** Microstructure of annealed SG cast iron without etching: (a) before the ECAP/E process, (b) the first region of specimen after the process and (c) the second region of specimen after the process.

Therefore:

$$\varepsilon_3 = -\frac{1}{(1 + \alpha)}\varepsilon_1 \quad (5)$$

As a result, equivalent plastic strain can be calculated as follows [20]:

$$\bar{\varepsilon} = \sqrt{\frac{2}{3}(\varepsilon_1^2 + \varepsilon_2^2 + \varepsilon_3^2)} = \sqrt{\frac{4(\alpha^2 + \alpha + 1)}{3(\alpha^2 + 2\alpha + 1)}} \varepsilon_1 = f(\alpha)\varepsilon_1 \quad (6)$$

Considering the aspect ratio of a graphite particle as below:

$$\beta = b/a \quad (7)$$

the aspect ratio of any graphite particle can be associated to the imposed equivalent plastic strain on that particle as below:

$$\ln(\beta) = \ln\left(\frac{b}{a}\right) = \ln\left(\frac{b}{d}\right) - \ln\left(\frac{a}{d}\right) = \varepsilon_1 - \varepsilon_3 = \frac{2 + \alpha}{1 + \alpha}\varepsilon_1 = \frac{2 + \alpha}{f(\alpha)(1 + \alpha)}\bar{\varepsilon} \quad (8)$$

Therefore, it can be seen that:

$$\bar{\varepsilon} = \frac{f(\alpha)(1 + \alpha)}{2 + \alpha}\ln(\beta) = g(\alpha)\ln(\beta) \quad (9)$$

Considering that  $\alpha$  is zero for the plane strain formulation and one for the axisymmetric strain formulation, the amounts of  $g(\alpha)$  for these formulation are calculated equal to 0.577 and 0.667, respectively. Regarding that strain field imposed using the applied ECAP/E process is between two mentioned formulations, one may consider the amount of  $g(\alpha)$  for the used ECAP/E process equal to  $0.62 \pm 0.05$ . Combining equation (9) with results of image processing on several hundreds of graphite particles shown in figure 5, the averages of imposed equivalent plastic strain on the first and the second regions of annealed specimen are calculated about  $0.9 \pm 0.07$  and  $0.44 \pm 0.04$ , respectively. These numbers are very close to results of previous studies on

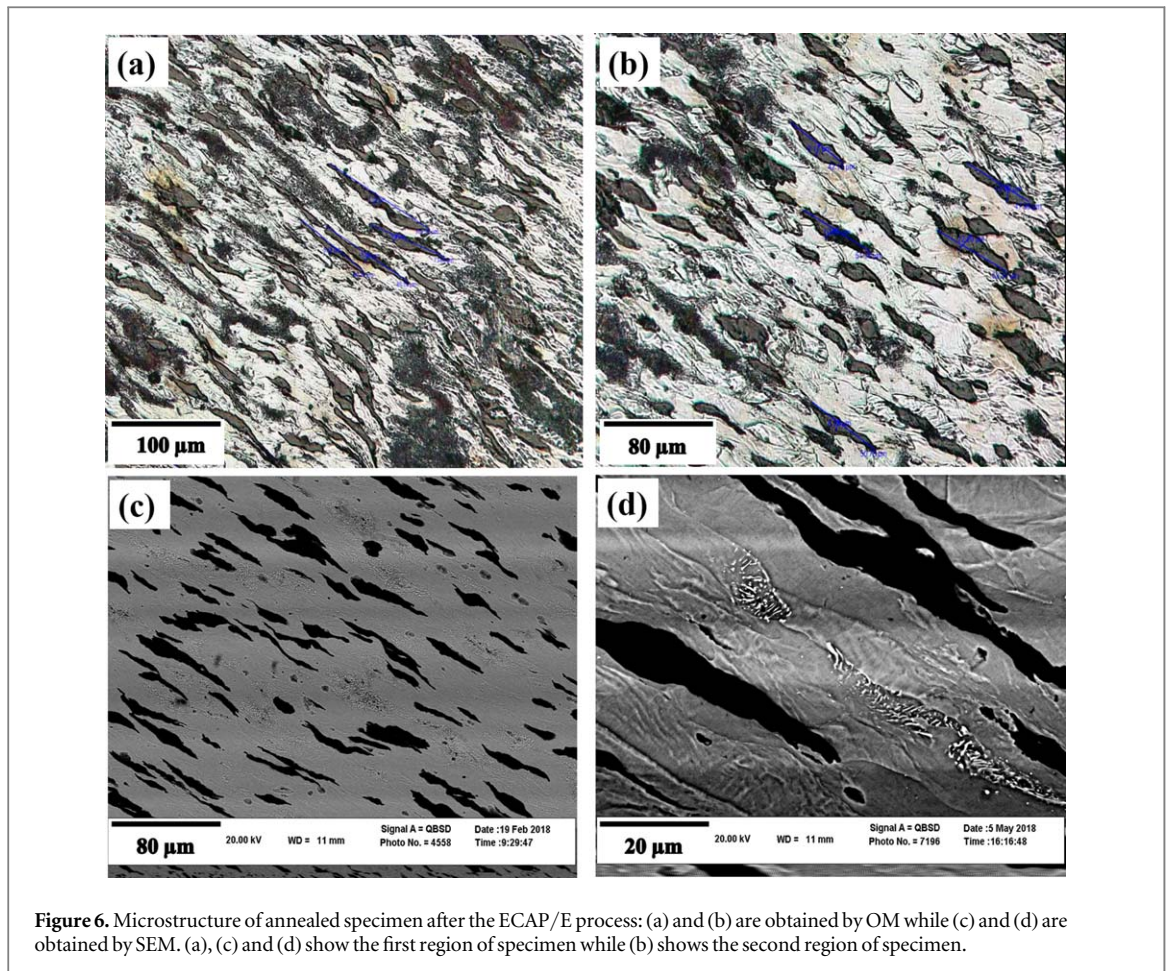


**Figure 6.** Microstructure of annealed specimen after the ECAP/E process: (a) and (b) are obtained by OM while (c) and (d) are obtained by SEM. (a), (c) and (d) show the first region of specimen while (b) shows the second region of specimen.

**Table 2.** Hardness of annealed specimen after imposition of different plastic strains.

Imposed plastic strain	0	0.44	0.9
Rockwell A hardness ( $\text{Kg mm}^{-2}$ )	54.5	62	64.5

calculation of equivalent plastic strain imposed on a cylindrical rod by the ECAP/E process [18, 19]. In addition, it is notable that imposition of this remarkable plastic strain on SG cast iron through a warm deformation regime has been rarely reported.

Figure 6 shows the microstructure of annealed specimen after the ECAP/E process. As can be seen here, the ECAP/E process results in stretching of ferrite grains. In addition, it is notable that the stretching of ferrite grains is more significant in the first region of specimen in comparison of its second region. This result is in agreement with what seen for graphite particles indicating to imposition of more severe plastic strain on the first region of specimen as discussed above. This effect is related to the used geometry of ECAP/E die which imposes less plastic strain at the initiation of the process [18, 19]. It is also notable that although the shapes of all graphite particles before the process are almost spheroidal, the shapes of graphite particles after the process are completely different from each other. Considering the presence of pearlite phase inside the microstructure of annealed specimen, one may relate this difference of shapes of graphite particles to a heterogeneous distribution of imposed plastic strain due to more strength of the pearlite phase. Note that the imposed plastic strain locally decreases around the pearlite phase while pearlite-free areas bear a more severe plastic strain [21, 22].

Table 2 compares hardness of the annealed specimen with imposed equivalent plastic strain through the ECAP/E process. As can be seen here, a considerable increase of hardness occurs due to imposition of plastic strain by the ECAP/E process. In addition, the increase of hardness with increase of imposed plastic strain is monotonic. This monotonic increase of hardness with increase of strain implies that dynamic recrystallization of the ferrite phase during the process does not occur. Note that the dynamic recrystallization results in appearance of strain softening which is in spite of monotonic increase of hardness with plastic strain. Consistently, the microstructure of annealed specimen after the process illustrated in figure 6 do not show any

evidence from occurrence of dynamic recrystallization of the ferrite phase. This result can be associated to the relatively low temperature of the ECAP/E processing. Note that although the imposed plastic strain through the ECAP/E process is absolutely enough for activation of dynamic recrystallization, the applied processing temperature is less than half of the melting temperature of iron which cannot be promising for occurrence of dynamic recrystallization [4, 23].

Comparing abovementioned results, one can infer that the SG cast iron can be severely strained at a warm deformation temperature whereas the effect of diffusional phenomena like dynamic recrystallization is limited. This enhanced workability of SG cast iron is owing to two factors. The first one is imposition of a compressive stress state through using of a suitable deformation process and application of a proper casing. The second one is application of an appropriate pre-annealing for appearance of a more ductile microstructure by significant decrease of fraction of pearlite.

## 4. Conclusion

Considering results of this work, it can be concluded that:

Using a proper casing and a suitable pre-annealing, the SG cast iron can be successfully subjected to the ECAP/E process at a temperature less than half of melting temperature of iron while no macroscopic fracture is seen after the process.

The microstructure of SG cast iron after the process consists of stretched graphite and ferrite phases while no evidence from occurrence of dynamic recrystallization of ferrite phase during the process is traced.

Using a simple model based on analyzing of aspect ratios of graphite particles after the process, the equivalent plastic strain imposed by the process is estimated about 0.9.

The enhanced workability of cast iron during the applied process is related to imposition of a compressive stress state as well as application of a pre-annealing.

## Acknowledgments

The authors wish to thank the research board of Ferdowsi University of Mashhad (FUM) for the financial support and the provision of research facilities used in this work through the grant number of 3/41498.

## ORCID iDs

M H Farshidi  <https://orcid.org/0000-0002-2454-3099>

## References

- [1] Labrecque C and Gagne M 1998 Ductile iron: fifty years of continuous development *Can. Metall. Quarter.* **37** 343–78
- [2] Angus H T 2013 *Cast Iron: Physical and Engineering Properties* (London: Butterworths) 9780408706889
- [3] Shcherbedinskii G V 2005 Iron: a promising material of the XXI century *Metal Sci. Heat Treat.* **47** 333–42
- [4] Sakai T, Belyakov A, Kaibyshev R, Miura H and Jonas JJ 2014 Dynamic and post-dynamic recrystallization under hot, cold and severe plastic deformation conditions *Prog. Mater. Sci.* **60** 130–207
- [5] Semiatin S L and Jonass J J 1984 *Formability and workability of metals: plastic instability and flow localization* (ASM series in metal processing 2) (Ohio: American Society for Metals) 9780871701831
- [6] Zhao X, Jing T F, Gao Y W, Zhou J F and Wang W 2004 A new SPD process for spheroidal cast iron *Mater. Lett.* **58** 2335–9
- [7] Chaus A S, Sojkaa J and Pokrovskii A I 2013 Effect of hot plastic deformation on microstructural changes in cast iron with globular graphite *Phys. Metal. Metallograph.* **114** 85–94
- [8] Lyakishev N P and Shcherbedinskii G V 2001 Hot plastic deformation of high-strength cast iron *Metal Sci Heat Treat.* **43** 421–2
- [9] Xin Z, Xiao-ling Y and Tian-fu J 2011 Processing maps for use in hot working of ductile iron *J. Iron Steel Research Int.* **18** 48–51
- [10] Qi K, Yu F, Bai F, Yan Z, Wang Z and Li T 2009 Research on the hot deformation behavior and graphite morphology of spheroidal graphite cast iron at high strain rate *Mater. Des.* **30** 4511–5
- [11] Calcagnotto M, Ponge D and Raabe D 2010 Effect of grain refinement to 1  $\mu\text{m}$  on strength and toughness of dual-phase steels *Mater. Sci. Eng. A* **527** 7832–40
- [12] Murty S V S N, Torizuka S, Nagai K, Kitai T and Kogo Y 2005 Dynamic recrystallization of ferrite during warm deformation of ultrafine grained ultra-low carbon steel *Scrip. Mater.* **53** 763–8
- [13] Bai Y and Wierzbicki T 2008 A new model of metal plasticity and fracture with pressure and Lode dependence *Int. J. Plast.* **24** 1071–96
- [14] Bao Y and Wierzbicki T 2005 On the cut-off value of negative triaxiality for fracture *Eng. Fract. Mech.* **72** 1049–69
- [15] Estrin Y and Vinogradov A 2013 Extreme grain refinement by severe plastic deformation: a wealth of challenging science *Acta Mater.* **61** 782–817

- [16] Zhao X, Fu W, Yang X and Langdon T G 2008 Microstructure and properties of pure titanium processed by equal-channel angular pressing at room temperature *Scrip. Mater.* **59** 542–5
- [17] Figueiredo R B, Cetlin P R and Langdon T G 2007 The processing of difficult-to-work alloys by ECAP with an emphasis on magnesium alloys *Acta Mater.* **55** 4769–79
- [18] Shaeri M H, Djavanroodi F, Sedighi M, Ahmadi S, Salehi M T and Seyyedein S H 2013 Effect of copper tube casing on strain distribution and mechanical properties of Al-7075 alloy processed by equal channel angular pressing *J. Strain Anal. Eng. Des.* **48** 512–21
- [19] Lee H H, Kim W, Jung K C, Seo S, Lee J K, Park H L, Park K T and Kim H S 2018 Circumferential twisting during route B equal-channel angular pressing *J Mater. Proc. Tech.* **259** 305–11
- [20] Hosford W F and Caddell R M 2007 *Metal Forming; Mechanics and Metallurgy* (Cambridge: Cambridge University Press) (<https://doi.org/10.1017/CBO9780511811111>)
- [21] Tasan C C *et al* 2015 An overview of dual-phase steels: advances in microstructure-oriented processing and micromechanically guided design *Annu. Rev. Mater. Res.* **45** 391–431
- [22] Nicoletto G, Collini L, Konecna R and Bujnova P 2005 Strain heterogeneity and damage localization in nodular cast iron microstructures *Mater. Sci. Forum* **482** 255–8
- [23] Ohmori A, Torizuka S, Nagai K, Koseki N and Kogo Y 2004 Effect of deformation temperature and strain rate on evolution of ultrafine grained structure through single-pass large-strain warm deformation in a low carbon steel *Mater. Transact.* **45** 2224–31